

1 *Supplementary Material*

2 **Phytoplankton temporal strategies increase entropy** 3 **production in marine a food web model**

4 **Joseph Vallino ^{1*} and Ioannis Tsakalakis ²**

5 ¹ Marine Biological Laboratory; jvallino@mbl.edu

6 ² Marine Biological Laboratory and Massachusetts Institute of Technology; itsakalakis@mbl.edu

7 * Correspondence: jvallino@mbl.edu

8 Received: date; Accepted: date; Published: date

9 **S1. Overview**

10 This *Supplementary Material* describes the details of the model used to demonstrate how temporal
11 strategies can increase entropy production over a given time interval. Constituent transport is
12 governed by a simple well-mixed chemostat-like pond of constant volume that receives a constant
13 flow of water with defined input concentrations and is illuminated at the surface with
14 monochromatic light (blue, 440 nm) that varies on both diel and seasonal cycles. The food web
15 consists of three functional groups, phytoplankton, S_P , bacteria, S_B , and consumers, S_C , that
16 produce or consume dissolved inorganic carbon, H_2CO_3 , oxygen, O_2 , ammonium, NH_3 , labile organic
17 carbon, C_L , and detrital organic carbon and nitrogen, C_D and N_D , respectively (Figure 1). Biological
18 structures for all three functional groups are given the same unit-carbon elemental composition,
19 $CH_{\alpha_S}O_{\beta_S}N_{\gamma_S}P_{\delta_S}$, but phytoplankton also contain an internal pool of carbon, C_P , with elemental
20 composition CH_2O . All concentrations are in $[[mmol\ m^{-3}]]$, where double brackets are used to
21 indicate units of variables. The model uses a trait-based approach [1] where each functional group,
22 $S_{\chi(i)}$, is represented by n_{χ} ecotypes, or realizations, that are assigned different parameter values that
23 govern reaction stoichiometries, growth kinetics and protein allocation to metabolic pathways, where
24 χ is either P , B or C . Unlike canonical trait-based models, parameters governing traits (aka control
25 variables [2]) for each ecotype are not randomly assigned but determined by solving a non-linear
26 optimization problem that maximizes integrated entropy production associated with irreversible
27 processes over a fixed simulation period of two years.

28 **S2. Transport, Reaction and Entropy Production Model**

29 *S2.1 Mass Balance model*

30 The maximum entropy production (MEP)-optimize trait-based model uses a simple 0D, well-
31 mixed system for transport, where nutrients and low concentrations of organisms flow into a
32 reservoir of volume V $[[m^3]]$ at flow rate F $[[m^3\ d^{-1}]]$ to produce a dilution rate of D $[[d^{-1}]] = \frac{F}{V}$. The
33 pond-like cylindrical reservoir is in contact with the atmosphere at one end, has a cross-sectional area
34 A $[[m^2]]$ and depth ζ_d $[[m]]$ and is illuminated at the surface with photosynthetically active radiation
35 (PAR) of intensity $I_0(t)$ $[[mmol\ photons\ m^{-2}\ d^{-1}]]$ that varies both diurnally and seasonally [3]. A
36 simple mass balance around the state variables leads to an initial value problem, which, in vector
37 form, is as follows,
38

$$\frac{d\mathbf{c}(t)}{dt} = D(\mathbf{c}^I - \mathbf{c}(t)) + \frac{A}{V} \mathbf{v} \circ (\mathbf{p} \circ \mathbf{h}(T) - \mathbf{c}(t)) + \mathbf{S}(\mathbf{u})\mathbf{r}(t; \mathbf{u}); \quad \left. \frac{d\mathbf{c}(t)}{dt} \right|_{t=t_0} = \mathbf{c}^I, \quad (S1)$$

39

40 where $\mathbf{c}(t) \in \mathbb{R}^{n_S}$ is a state vector of n_S concentration variables $[[mmol\ m^{-3}]]$ given by,
 41

$$\mathbf{c}^T(t) = \begin{bmatrix} c_{H_2CO_3} & c_{O_2} & c_{NH_3} & c_{C_L} & c_{C_D} & c_{N_D} & c_{S_{P\{1\}}} & \dots & c_{S_{P\{n_P\}}} & c_{C_{P\{1\}}} & \dots & c_{C_{P\{n_P\}}} \\ c_{S_{B\{1\}}} & \dots & c_{S_{B\{n_B\}}} & c_{S_{C\{1\}}} & \dots & c_{S_{C\{n_C\}}} \end{bmatrix}, \quad (S2)$$

42
 43
 44 that consists of 6 chemical constituents, n_P phytoplankton ecotypes with associated n_P internal C_P
 45 storage pool, n_B bacteria ecotypes and n_C consumer ecotypes so that $n_S = 6 + 2n_P + n_B + n_C$; \mathbf{c}^I
 46 are the input concentrations that also serve as the initial conditions at t_0 ; a stagnant-film model
 47 governs mass exchange across the air-water interface for state variables with gas phases (CO_2 and
 48 O_2), where $\mathbf{v} [[m\ d^{-1}]]$ is the piston velocity, $\mathbf{p} [[Pa]]$ is atmospheric gas partial pressure and $\mathbf{h}(T)$ is
 49 the Henry's law coefficient $[[mmol\ m^{-3}\ Pa^{-1}]]$ at temperature $T [[K]]$, and \circ is the element-wise
 50 multiplication (Hadamard) operator; $\mathbf{r}(t; \mathbf{u}) \in \mathbb{R}^{n_r}$ is a vector of n_r reaction rates $[[mmol\ m^{-3}\ d^{-1}]]$
 51 associated with biological structures (see below) and $\mathbf{S}(\mathbf{u}) \in \mathbb{R}^{n_S \times n_r}$ is a reaction stoichiometry
 52 matrix. Reaction rates and the stoichiometric matrix depend on a time-invariant control vector, \mathbf{u} ,
 53 that consists of a vector of reaction efficiencies, $\boldsymbol{\varepsilon}$, and a vector of resource allocation controls, $\boldsymbol{\Omega}$,
 54 ($\mathbf{u}^T = [\boldsymbol{\varepsilon}^T\ \boldsymbol{\Omega}^T]$) described in Section S2.2. In this formulation, the control variables, $\boldsymbol{\Omega}$ and $\boldsymbol{\varepsilon}$, are held
 55 constant for each ecotype, so serve as the trait variables.

56 S2.2 Metabolic Reaction Rates

57 The metabolic reactions associated with phytoplankton, bacteria and consumers (grazers)
 58 follows that developed previously [2], except in this implementation each functional group can have
 59 a specified number of ecotypes that have different values for the control variables (i.e., traits). We
 60 use braces, $\{i\}$, to designate each realization of an ecotype defined by the trait values and χ
 61 represents one of the three functional groups (P, B or C). The governing equations for each of the
 62 three functional groups are given below, with the following overall organization. The metabolic
 63 reactions a functional group is capable of catalyzing includes a thermodynamic efficiency trait, $\varepsilon_{\chi\{i\}}$,
 64 that specifies weighting between an anabolic (i.e., biosynthesis) reaction and a catabolic (energy
 65 producing) reaction. The anabolic and catabolic reactions are combined into a single reaction and
 66 balanced with the parameter $n_{j,\chi\{i\}}$ that ensures as $\varepsilon_{\chi\{i\}}$ approaches 1, the Gibbs free energy of
 67 reaction goes to 0, so the reaction is at equilibrium. The anabolic and catabolic reactions given below
 68 can be recovered by setting $n_{j,\chi\{i\}}$ to 0 and setting $\varepsilon_{\chi\{i\}}$ to 1 or 0, respectively. Reaction entropy is
 69 maximized as $\varepsilon_{\chi\{i\}}$ approaches 0, as this represents complete conversion of free energy to heat.
 70 Stoichiometric coefficients, such as $a_{j,P}^A$ and $b_{j,B}^C$, are used to balance O and H, respectively, where
 71 the superscript is for either the anabolic (A) or catabolic (C) reaction, and the subscripts correspond
 72 to the reaction number, j , for the associated functional group (P, B or C). Defined by whole reaction
 73 stoichiometry, the Gibbs free energy of reaction, $\Delta_r G$, accounts for the reaction quotient, and the
 74 standard Gibbs free energy of reaction, $\Delta_r G^\circ$, is obtained from Alberty's [4] that accounts for
 75 ionization of chemical species based on pH and temperature, and ionic strength is used to
 76 approximate activity from concentration. Reaction kinetics are based on an adaptive Monod equation
 77 [2] that consists of a kinetic driver, F_K , that is parameterized by $\varepsilon_{\chi\{i\}}$ and also includes a
 78 thermodynamic driver, F_T , that depends on the number of electrons, $n_{j,\chi\{i\}}^e$, transferred in the
 79 catabolic reaction as described by LaRowe et al. [5]. Bracket notation, $[]$, is used to represent
 80 concentration of state variables (i.e., $[NH_3]$ and c_{NH_3} are equivalent). The fraction of biological
 81 structure allocated to each metabolic reaction that a functional group can catalyzed is determined by
 82 $\Omega_{j,\chi\{i\}}$, where $\sum_j \Omega_{j,\chi\{i\}} = 1$ and $0 \leq \Omega_{j,\chi\{i\}} \leq 1 \forall j$ because the total catalytic capacity is constrained
 83 by the concertation of biological structure, $[S_{\chi\{i\}}]$, that changes over time. Entropy production is
 84 calculated for dissipation of chemical free energy by metabolic reactions, $\dot{\sigma}_{j,\chi\{i\}}^R$, as well as dissipation
 85 of electromagnetic free energy by particulate material, $\dot{\sigma}_{j,\chi\{i\}}^P$, and water, $\dot{\sigma}^W$, although the latter does
 86 not depend on any of the state variables, so is not listed below (See Section S2.4 below). We use $R_{j,\chi\{i\}}$

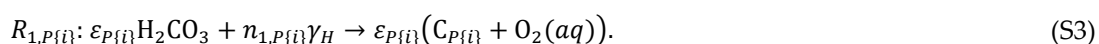
87 to refer to the stoichiometry of reaction j catalyzed by biological structure $S_{\chi\{i\}}$, and $r_{j,\chi\{i\}}$ for the
88 reaction rate.

89 S2.2.1 Phytoplankton Reactions

90 Phytoplankton are represented with two metabolic reactions consisting of 1) $R_{1,P\{i\}}$, CO₂ fixation
91 into unit-C sugar (i.e. CH₂O, or $C_{P\{i\}}$) driven by high frequency photon, γ_H , capture and 2) $R_{2,P\{i\}}$,
92 conversion of $C_{P\{i\}}$ into biomass using available ammonium and phosphate driven by the catabolic
93 aerobic oxidation of $C_{P\{i\}}$. (Note, phosphate is not a state variable and is held at a fixed concentration
94 of 1 μ M during simulations.) Surficial light intensity, $I_0(t)$, varies on both diel and seasonal cycles
95 [3], and depth-average light intensity, $\langle I(t) \rangle_{\zeta_d}$, for the well-mixed system is calculated from $I_0(t)$
96 and light at depth ζ_d , where light attenuation occurs by water, particle and chlorophyll a absorption
97 as parameterized by k_w , k_p and k_{chl} respectively. We only consider blue light at 440 nm and the
98 light attenuation coefficients, k_w , k_p and k_{chl} were derived from Wozniak [6] and set to 0.011 m⁻¹,
99 0.000625 m² (mmol-C)⁻¹ and 0.0025 m² (mmol-C)⁻¹ for 440 nm light, respectively, after conversion to
100 mM C. The Gibbs free energy of photons, $\Delta_r G_\gamma$, at 440 nm is -253 J (mmol- γ)⁻¹, which accounts for
101 the conversion of photons to work [2,7]. Entropy production for phytoplankton is divided into
102 reaction associated, $\dot{\sigma}_{1,P\{i\}}^R$, and particle absorption, $\dot{\sigma}_{1,P\{i\}}^P$, components that are controlled by $\Omega_{1,P\{i\}}$
103 and $\Omega_{2,P\{i\}}$. Light absorbed by water and non-photosynthetic biomass, $\Omega_{2,P\{i\}}[S_{P\{i\}}]$, is simply
104 dissipated as heat and contributes to entropy production. Only the fraction of electromagnetic free
105 energy that is converted to chemical potential (i.e., $C_{P\{i\}}$ and $S_{P\{i\}}$ synthesis) does not contribute to
106 entropy production (see Eqn. (S13) for $\dot{\sigma}_{1,P\{i\}}^T$ below). The fraction of phytoplankton biomass
107 allocated to photosynthetic processes described by $R_{1,P\{i\}}$ is given by $\Omega_{1,P\{i\}}[S_{P\{i\}}]$; however, since
108 the photosynthetic machinery can be kinetically limited by resource availability (i.e., [CO₂] +
109 [HCO₃⁻]) or thermodynamics, F_T , only the fraction of the total photon capture rate that contributes to
110 $r_{1,P\{i\}}$, given by $\frac{\Delta I_{P\{i\}}}{n_{1,P\{i\}}}$, contributes to $\dot{\sigma}_{1,P\{i\}}^R$, while the remainder contributes to $\dot{\sigma}_{1,P\{i\}}^P$. That is, if the
111 photosynthetic machinery is constrained, the excess light captured is dissipated as heat, so
112 contributes to $\dot{\sigma}_{1,P\{i\}}^P$. Light intercepted by biological structure allocated to biosynthesis, given by
113 $\Omega_{2,P\{i\}}[S_{P\{i\}}]$, always contributes to particle-associated entropy production, while dissipation of
114 chemical free energy associated with catabolic reactions contributes to reaction-associated entropy
115 production, $\dot{\sigma}_{2,P\{i\}}^R$. For the carbon dioxide fixation reaction ($R_{1,P\{i\}}$, Eq. (S3)), $n_{1,P\{i\}}$ is the moles of
116 high frequency photons, γ_H , needed to fix one mole of CO₂, reversibly, under the current conditions,
117 so that the quantum yield, $\frac{n_{1,P\{i\}}}{\varepsilon_{P\{i\}}}$, depends on $\varepsilon_{P\{i\}}$. The concentration of fixed carbon, $[C_{P\{i\}}]$, is based
118 on total system volume, but for kinetics it is treated as an intracellular component, so is multiplied
119 by a system-to-cell volume factor, φ_f , to reflect its higher intracellular concentration (φ_f was set to
120 1000 for all simulations). Below are the equations describing phytoplankton growth and associated
121 entropy production.

123 Carbon dioxide fixation driven by solar radiation: $R_{1,P\{i\}}$

124 Overall stoichiometry of reaction $R_{1,P\{i\}}$ containing catabolic and anabolic sub-reactions,



125 The free energy needed to fix H₂CO₃ into $C_{P\{i\}}$ (unit carbon glucose) and O₂ (anabolic sub-
126 reaction) is given by,

$$\Delta_r G_{C_{P\{i\}}}^o = \Delta_f G_{\text{CH}_2\text{O}}^o + \Delta_f G_{\text{O}_2(aq)}^o - \Delta_f G_{\text{H}_2\text{CO}_3}^o, \quad (\text{S4})$$

$$\Delta_r G_{C_{P\{i\}}} = \Delta_r G_{C_{P\{i\}}}^o + RT \ln \left(\frac{[C_{P\{i\}}][\text{O}_2(aq)]}{[\text{H}_2\text{CO}_3]} \right). \quad (\text{S5})$$

127 The moles of photons with free energy $\Delta_r G_\gamma$ needed to produce one mole of $C_{P\{i\}}$ is given by,

$$n_{1,P\{i\}} = -\frac{\Delta_r G_{C_{P\{i\}}}}{\Delta_r G_\gamma}, \quad (S6)$$

128 where $n_{1,P\{i\}}/\varepsilon_{P\{i\}}$ is the quantum yield of photosynthesis.

129

130 The overall Gibbs free energy of reaction for $R_{1,P\{i\}}$ is then,

$$\Delta_r G_{1,P\{i\}} = -(1 - \varepsilon_{P\{i\}})\Delta_r G_{C_{P\{i\}}}. \quad (S7)$$

131 Light attenuation by water, particles and photosynthetic machinery (Chl a) is given by,

$$k_{wp} = k_w + k_p \left(\sum_i \Omega_{2,P\{i\}} [S_{P\{i\}}] + \sum_i [C_{P\{i\}}] + \sum_i [S_{B\{i\}}] + \sum_i [S_{C\{i\}}] \right) + k_{chl} \sum_i \Omega_{1,P\{i\}} [S_{P\{i\}}]. \quad (S8)$$

132 Average light intensity in a well-mixed reservoir of depth ζ_d is given by,

$$\langle I(t) \rangle_{\zeta_d} = \frac{I_0(t)(1 - e^{-k_{wp}\zeta_d})}{k_{wp}\zeta_d}, \quad (S9)$$

133 and the volumetric rate of photon capture by Chl a over depth ζ_d is,

$$\Delta I_{P\{i\}} = k_{chl} \Omega_{1,P\{i\}} [S_{P\{i\}}] \langle I(t) \rangle_{\zeta_d}. \quad (S10)$$

134 Electrons transfer in the catabolic sub-reaction of $R_{1,P\{i\}}$ is

$$n_{1,P\{i\}}^e = n_{1,P\{i\}}. \quad (S11)$$

135 Reaction rate of $R_{1,P\{i\}}$ is given by,

$$r_{1,P\{i\}} = \frac{\Delta I_{P\{i\}}}{n_{1,P\{i\}}} \left(\frac{[CO_2] + [HCO_3^-]}{[CO_2] + [HCO_3^-] + \kappa^* \varepsilon_{P\{i\}}^A} \right) F_T (\Delta_r G_{1,P\{i\}}, n_{1,P\{i\}}^e), \quad (S12)$$

136 where the term enclosed by () is the kinetic drive, F_K . Total entropy production from reaction
137 $R_{1,P\{i\}}$ and light absorption by photosynthetic apparatus of $S_{P\{i\}}$ is given by,

$$\dot{\sigma}_{1,P\{i\}}^T = \frac{A\zeta_d}{T} \Delta_r G_{C_{P\{i\}}} \left(\frac{\Delta I_{P\{i\}}}{n_{1,P\{i\}}} - \varepsilon_{P\{i\}} r_{1,P\{i\}} \right), \quad (S13)$$

138 which contributes to entropy production from reactions and particles as follows,

$$\dot{\sigma}_{1,P\{i\}}^R = r_{1,P\{i\}} \frac{n_{1,P\{i\}}}{\Delta I_{P\{i\}}} \dot{\sigma}_{1,P\{i\}}^T, \quad (S14)$$

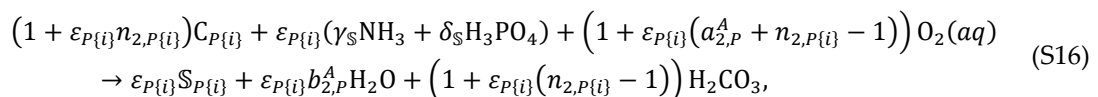
$$\dot{\sigma}_{1,P\{i\}}^P = \dot{\sigma}_{1,P\{i\}}^T - \dot{\sigma}_{1,P\{i\}}^R. \quad (S15)$$

139 Note, if $r_{1,P\{i\}}$ is unconstrained by F_K or F_T , then $\dot{\sigma}_{1,P\{i\}}^R = \dot{\sigma}_{1,P\{i\}}^T$ and $\dot{\sigma}_{1,P\{i\}}^P = 0$.

140

141 Conversion of fixed carbon into phytoplankton biomass: $R_{2,P\{i\}}$

142 Full stoichiometry of reaction $R_{2,P\{i\}}$ is given by,



143 where the stoichiometric coefficients to balance H and O are,

$$a_{2,P}^A = \frac{1}{4} (-\alpha_S + 2\beta_S + 3\gamma_S - 5\delta_S), \quad (S17)$$

$$b_{2,P}^A = \frac{1}{2} (2 - \alpha_S + 3\gamma_S + 3\delta_S). \quad (S18)$$

144 Free energy of reaction for the anabolic component of $R_{2,P\{i\}}$, $R_{2,P\{i\}}^A \stackrel{\text{def}}{=} C_{P\{i\}} + \gamma_S NH_3 +$
145 $\delta_S H_3 PO_4 + a_{2,P}^A O_2(aq) \rightarrow S_{P\{i\}} + b_{2,P}^A H_2 O$, is given by,

$$\Delta_r^A G_{2,P\{i\}}^o = (\Delta_f G_S^o + b_{2,P}^A \Delta_f G_{H_2O}^o) - (\Delta_f G_{C_{P\{i\}}}^o + \gamma_S \Delta_f G_{NH_3}^o + \delta_S \Delta_f G_{H_3PO_4}^o + a_{2,P}^A \Delta_f G_{O_2(aq)}^o), \quad (S19)$$

$$\Delta_r^A G_{2,P\{i\}} = \Delta_r^A G_{2,P\{i\}}^o + RT \ln \left(\frac{[S_{P\{i\}}]}{[C_{P\{i\}}][NH_3]^{\gamma_S}[H_3PO_4]^{\delta_S}[O_2(aq)]^{a_{2,P}^A}} \right). \quad (S20)$$

146 Free energy of reaction for catabolic component of $R_{2,P\{i\}}$, $R_{2,P\{i\}}^C \stackrel{\text{def}}{=} C_{P\{i\}} + O_2(aq) \rightarrow H_2CO_3$, is
147 given by,

$$\Delta_r^C G_{2,P\{i\}}^o = \Delta_f G_{H_2CO_3}^o - (\Delta_f G_{C_{P\{i\}}}^o + \Delta_f G_{O_2(aq)}^o), \quad (S21)$$

$$\Delta_r^C G_{2,P\{i\}} = \Delta_r^C G_{2,P\{i\}}^o + RT \ln \left(\frac{[H_2CO_3]}{[C_{P\{i\}}][O_2(aq)]} \right). \quad (S22)$$

148 In order to insure that $R_{2,P\{i\}}$ is at equilibrium when $\varepsilon_{P\{i\}} = 1$, the catabolic reaction, $R_{2,P\{i\}}^C$, is
149 added to the anabolic reaction, $R_{2,P\{i\}}^A$, so that the Gibbs free energy of reaction, $\Delta_r G_{2,P\{i\}}$, for
150 $R_{2,P\{i\}}$ equals zero. The coefficient $n_{2,P\{i\}}$ defines moles of $C_{P\{i\}}$ that need to be oxidized for this
151 to occur when $\varepsilon_{P\{i\}} = 1$, which is given by:

$$n_{2,P\{i\}} = -\frac{\Delta_r^A G_{2,P\{i\}}}{\Delta_r^C G_{2,P\{i\}}}. \quad (S23)$$

152 Consequently, the Gibbs free energy of reaction for $R_{2,P\{i\}}$ is,

$$\Delta_r G_{2,P\{i\}} = (1 - \varepsilon_{P\{i\}}) \Delta_r^C G_{2,P\{i\}}, \quad (S24)$$

153 and the electrons transferred in reaction $R_{2,P\{i\}}^C$ is given by,

$$n_{2,P\{i\}}^e = 4. \quad (S25)$$

154 Reaction rate of $R_{2,P\{i\}}$:

$$r_{2,P\{i\}} = v^* \varepsilon_{P\{i\}}^2 \Omega_{2,P\{i\}} [S_{P\{i\}}] \left(\frac{[C_{P\{i\}}] \varphi_f}{[C_{P\{i\}}] \varphi_f + \kappa^* \varepsilon_{P\{i\}}^4} \right) \left(\frac{[NH_3]/\gamma_S}{[NH_3]/\gamma_S + \kappa^* \varepsilon_{P\{i\}}^4} \right) \times \left(\frac{[O_2]}{[O_2] + \kappa^* \varepsilon_{P\{i\}}^4} \right) F_T(\Delta_r G_{2,P\{i\}}, n_{2,P\{i\}}^e), \quad (S26)$$

155 where again the kinetic drive is comprised of the terms in (). Entropy production from
156 reaction $R_{2,P\{i\}}$ and light absorption by the biosynthetic fraction of $S_{P\{i\}}$ biomass is given by,

$$\dot{\sigma}_{2,P\{i\}}^R = -\frac{A \zeta_d}{T} r_{2,P\{i\}} \Delta_r G_{2,P\{i\}}, \quad (S27)$$

$$\dot{\sigma}_{2,P\{i\}}^P = -\frac{A \zeta_d}{T} \langle I(t) \rangle_d \Delta_r G_{\gamma} k_p \Omega_{2,P\{i\}} [S_{P\{i\}}]. \quad (S28)$$

157

158 S2.2.2 Bacteria growth on labile carbon, C_L

159 Bacteria catalyze three reactions that include growth on labile carbon, C_L , and decomposition of
160 detrital carbon, C_D , and nitrogen, N_D , into labile pools, where $\Omega_{1,B\{i\}}$, $\Omega_{2,B\{i\}}$ and $\Omega_{3,B\{i\}}$ determine
161 the allocation of catalytic machinery to each reaction, respectively. Decomposition of detritus, which
162 is recalcitrant, uses a different biomass-specific rate constant, v_D^* , than that used for growth on labile
163 carbon. Note, the formulation for $R_{1,B\{i\}}$ differs slightly from that for phytoplankton, $R_{2,B\{i\}}$, in that
164 the anabolic reaction is not exactly balanced by a small amount of the catabolic reaction when $\varepsilon_{B\{i\}} =$
165 1, so that $\Delta_r G_{1,B\{i\}}$ is slightly less than 0 when $\varepsilon_{B\{i\}} = 1$. Instead, a sufficient amount of labile carbon,
166 C_L , given by $a_{1,B}^A$, is converted to CO_2 to balance O in $R_{1,B\{i\}}$. This slightly different formulation was
167 used to be consistent with previous work [2], but we have found the two different approaches
168 produce the same numerical results.

169

170 **Bacterial growth:** $R_{1,B\{i\}}$ 171 Stoichiometry of reaction $R_{1,B\{i\}}$ and coefficients to balance H and O are given by,

$$C_L + \varepsilon_{B\{i\}}(\gamma_S NH_3 + \delta_S H_3 PO_4) + (1 - \varepsilon_{B\{i\}})O_2(aq) \\ \rightarrow \varepsilon_{B\{i\}} a_{1,B}^A S_{B\{i\}} + (2 - \varepsilon_{B\{i\}}(a_{1,B}^A + 1)) H_2 CO_3 + \varepsilon_{B\{i\}} b_{1,B}^A H_2 O, \quad (S29)$$

$$a_{1,B}^A = \frac{4 + 3\gamma_S - 5\delta_S}{4 + \alpha_S - 2\beta_S}, \quad (S30)$$

$$b_{1,B}^A = \frac{4 - 2\alpha_S + 9\gamma_S - 3\beta_S\gamma_S + \delta_S + 4\alpha_S\delta_S - 3\beta_S\delta_S}{4 + \alpha_S - 2\beta_S}. \quad (S31)$$

172 Gibbs free energy of reaction for anabolic and catabolic components of $R_{1,B\{i\}}$ are,

$$\Delta_r^A G_{1,B\{i\}}^o \\ = (\alpha_{1,B}^A \Delta_f G_S^o + (1 - \alpha_{1,B}^A) \Delta_f G_{H_2CO_3}^o + b_{1,B}^A \Delta_f G_{H_2O}^o) \\ - (\Delta_f G_{C_L}^o + \gamma_S \Delta_f G_{NH_3}^o + \delta_S \Delta_f G_{H_3PO_4}^o), \quad (S32)$$

$$\Delta_r^A G_{1,B\{i\}} = \Delta_r^A G_{1,B\{i\}}^o + RT \ln \left(\frac{[S_{B\{i\}}]^{a_{1,B}^A} [H_2CO_3]^{(1-a_{1,B}^A)}}{[C_L][NH_3]^{\gamma_S} [H_3PO_4]^{\delta_S}} \right), \quad (S33)$$

$$\Delta_r^C G_{1,B\{i\}}^o = \Delta_f G_{H_2CO_3}^o - (\Delta_f G_{C_L}^o + \Delta_f G_{O_2(aq)}^o), \quad (S34)$$

$$\Delta_r^C G_{1,B\{i\}} = \Delta_r^C G_{1,B\{i\}}^o + RT \ln \left(\frac{[H_2CO_3]}{[C_L][O_2(aq)]} \right). \quad (S35)$$

173 Overall Gibbs free energy of reaction for $R_{1,B\{i\}}$ is,

$$\Delta_r G_{1,B\{i\}} = \varepsilon_{B\{i\}} \Delta_r^A G_{1,B\{i\}} + (1 - \varepsilon_{B\{i\}}) \Delta_r^C G_{1,B\{i\}}. \quad (S36)$$

174 Note, in this formulation $\Delta_r G_{1,B\{i\}}$ equals $\Delta_r^A G_{1,B\{i\}}$ when $\varepsilon_{B\{i\}} = 1$, which is not exactly 0 as was
175 formulated for the phytoplankton biosynthetic reaction, but it is typically close to 0.

176

177 Electrons transferred in catabolic portion of reaction $R_{1,B\{i\}}$ are,

$$n_{1,B\{i\}}^e = 4, \quad (S37)$$

178 And the reaction rate, $r_{1,B\{i\}}$, of $R_{1,B\{i\}}$ is,

$$r_{1,B\{i\}} = \nu^* \varepsilon_{B\{i\}}^2 \Omega_{1,B\{i\}} [S_{B\{i\}}] \left(\frac{[C_L]}{[C_L] + \kappa^* \varepsilon_{B\{i\}}^4} \right) \left(\frac{[NH_3]/\gamma_S}{[NH_3]/\gamma_S + \kappa^* \varepsilon_{B\{i\}}^4} \right) \\ \times \left(\frac{[O_2]}{[O_2] + \kappa^* \varepsilon_{B\{i\}}^4} \right) F_T(\Delta_r G_{1,B\{i\}}, n_{1,B\{i\}}^e). \quad (S38)$$

179 Entropy production from reaction $R_{1,B\{i\}}$ and light absorption by the fraction of $S_{B\{i\}}$ biomass
180 allocated to reaction $R_{1,P\{i\}}$ is given by,

$$\dot{\sigma}_{1,B\{i\}}^R = -\frac{A_d^Z}{T} r_{1,B\{i\}} \Delta_r G_{1,B\{i\}} \text{ and} \quad (S39)$$

$$\dot{\sigma}_{1,B\{i\}}^P = -\frac{A_d^Z}{T} \langle I(t) \rangle_a \Delta_r G_{\gamma} k_p \Omega_{1,B\{i\}} [S_{B\{i\}}]. \quad (S40)$$

181

182 **Bacterial decomposition of recalcitrant carbon:** $R_{2,B\{i\}}$ 183 Stoichiometry of reaction $R_{2,B\{i\}}$ is,

$$C_D \rightarrow C_L, \quad (S41)$$

184 where the Gibbs free energy of reaction for $R_{2,B\{i\}}$ due to concentration differences is,

$$\Delta_r G_{2,B\{i\}} = RT \ln \left(\frac{[C_L]}{[C_D]} \right). \quad (S42)$$

185 The reaction rate, $r_{2,B\{i\}}$, for $R_{2,B\{i\}}$ is given by,

$$r_{2,B\{i\}} = v_D^* \varepsilon_{B\{i\}}^2 \Omega_{2,B\{i\}} [S_{B\{i\}}] \left(\frac{[C_D]}{[C_D] + \kappa^* \varepsilon_{B\{i\}}^4} \right), \text{ for } \Delta_r G_{2,B\{i\}} < 0; 0 \text{ otherwise.} \quad (S43)$$

186 Entropy production from reaction $R_{2,B\{i\}}$ and light absorption by $\Omega_{2,B\{i\}} [S_{B\{i\}}]$ is,

$$\dot{\sigma}_{2,B\{i\}}^R = -\frac{A \zeta_d}{T} r_{2,B\{i\}} \Delta_r G_{2,B\{i\}} \text{ and} \quad (S44)$$

$$\dot{\sigma}_{2,B\{i\}}^P = -\frac{A \zeta_d}{T} \langle I(t) \rangle_d \Delta_r G_{\gamma} k_p \Omega_{2,B\{i\}} [S_{B\{i\}}]. \quad (S45)$$

187

188 **Bacterial decomposition of recalcitrant nitrogen:** $R_{3,B\{i\}}$

189 The reaction rate and entropy production associated with $R_{3,B\{i\}}$ are similar to that for $R_{2,B\{i\}}$,
190 except $R_{3,B\{i\}}$ governs the breakdown of N_D to NH_3 as described by:



$$\Delta_r G_{3,B\{i\}} = RT \ln \left(\frac{[NH_3]}{[N_D]} \right), \quad (S47)$$

$$r_{3,B\{i\}} = v_D^* \varepsilon_{B\{i\}}^2 \Omega_{3,B\{i\}} [S_{B\{i\}}] \left(\frac{[N_D]}{[N_D] + \kappa^* \varepsilon_{Bac}^4} \right), \text{ for } \Delta_r G_{3,B\{i\}} < 0; 0 \text{ otherwise,} \quad (S48)$$

$$\dot{\sigma}_{3,B\{i\}}^R = -\frac{A \zeta_d}{T} r_{3,B\{i\}} \Delta_r G_{3,B\{i\}}, \quad (S49)$$

$$\dot{\sigma}_{3,B\{i\}}^P = -\frac{A \zeta_d}{T} \langle I(t) \rangle_d \Delta_r G_{\gamma} k_p \Omega_{3,B\{i\}} [S_{B\{i\}}]. \quad (S50)$$

191

192 S2.2.3 Consumer predation rate, $R_{\chi\{j\},C\{i\}}$

193 Consumers prey on all function groups including themselves (i.e., cannibalism). We use nearly
194 the same governing equations as before [2], where C in biological structure is converted into biomass,
195 H_2CO_3 and detrital carbon; however, all $C_{P\{i\}}$ storage in phytoplankton is oxidized to H_2CO_3 instead
196 of being excreted as C_L . Excess N and P from consumed biological structure is excreted in both labile
197 and detrital forms as a function of $\varepsilon_{C\{i\}}$. The rationale is that when a consumer grows with high
198 thermodynamic efficiency ($\varepsilon_{C\{i\}}$ closer to 1), prey are processed more effectively leading to NH_3 and
199 H_3PO_4 production, while low efficiency growth leads to more detrital products. This version also
200 weights allocation to prey consumption normalized by prey density, as given by $\omega_{\chi\{j\},C\{i\}}$ below;
201 consequently, no constraint is placed on the sum, $\sum_j \Omega_{\chi\{j\},C\{i\}}$, as it is for phytoplankton and bacteria
202 (in theory, one degree of freedom could be removed though). In the equations below, the subscript
203 $\chi\{j\}$ represented any ecotype, $\{j\}$, of any of the three functional groups, where χ can be P, B or C,
204 and $[C_{\chi\{j\}}]$ equals 0 when χ is equal to B or C, since those functional groups have no internal carbon
205 storage in this version of the model.

206

207 Stoichiometry of reaction $R_{\chi\{j\},C\{i\}}$ and coefficients to balance O and H are given by,

$$\begin{aligned}
& S_{\chi\{j\}} + \frac{[C_{\chi\{j\}}]}{[S_{\chi\{j\}}]} C_{\chi\{j\}} + \left(a_{C\{i\}}^c (1 - \varepsilon_{C\{i\}}) + \frac{[C_{\chi\{j\}}]}{[S_{\chi\{j\}}]} \right) O_2(aq) \\
& \rightarrow \varepsilon_{C\{i\}} S_{C\{i\}} + (1 - \varepsilon_{C\{i\}}) \left((1 - \varepsilon_{C\{i\}}) H_2CO_3 + \varepsilon_{C\{i\}} C_D \right) \\
& + \gamma_S (1 - \varepsilon_{C\{i\}}) \left((1 - \varepsilon_{C\{i\}}) NH_3 + \varepsilon_{C\{i\}} N_D \right) \\
& + \delta_S (1 - \varepsilon_{C\{i\}}) \left((1 - \varepsilon_{C\{i\}}) H_3PO_4 + \varepsilon_{C\{i\}} P_D \right) + b_C^c (1 - \varepsilon_{C\{i\}}) H_2O \\
& + \frac{[C_{\chi\{j\}}]}{[S_{\chi\{j\}}]} H_2CO_3,
\end{aligned} \tag{S51}$$

$$a_{C\{i\}}^c = \frac{1}{4} (4 + \alpha_S - 2\beta_S - 3\gamma_S + 5\delta_S - 4\varepsilon_{C\{i\}}) \text{ and} \tag{S52}$$

$$b_C^c = \frac{1}{2} (-2 + \alpha_S - 3\gamma_S - 3\delta_S). \tag{S53}$$

208 Standard Gibbs free energy of reaction for $R_{\chi\{j\},C\{i\}}$ is given by,

$$\begin{aligned}
& \Delta_r G_{\chi\{j\},C\{i\}}^o \\
& = \left(\varepsilon_{C\{i\}} \Delta_f G_S^o + \left((1 - \varepsilon_{C\{i\}})^2 + \frac{[C_{\chi\{j\}}]}{[S_{\chi\{j\}}]} \right) \Delta_f G_{H_2CO_3}^o + \varepsilon_{C\{i\}} (1 - \varepsilon_{C\{i\}}) \Delta_f G_{C_D}^o \right. \\
& \left. + \delta_S (1 - \varepsilon_{C\{i\}}) \Delta_f G_{H_3PO_4}^o + \gamma_S (1 - \varepsilon_{C\{i\}}) \Delta_f G_{NH_3}^o + b_C^c (1 - \varepsilon_{C\{i\}}) \Delta_f G_{H_2O}^o \right) \\
& - \left(\Delta_f G_S^o + \left(a_{C\{i\}}^c (1 - \varepsilon_{C\{i\}}) + \frac{[C_{\chi\{j\}}]}{[S_{\chi\{j\}}]} \right) \Delta_f G_{O_2(aq)}^o + \frac{[C_{\chi\{j\}}]}{[S_{\chi\{j\}}]} \Delta_f G_{C_{H_2O}}^o \right),
\end{aligned} \tag{S54}$$

209 and the Gibbs free energy of reaction for $R_{\chi\{j\},C\{i\}}$ accounting for reaction quotient is,

$$\begin{aligned}
& \Delta_r G_{\chi\{j\},C\{i\}} \\
& = \Delta_r G_{\chi\{j\},C\{i\}}^o + RT \ln \left([S_{C\{i\}}]^{\varepsilon_{C\{i\}}} [H_2CO_3]^{(1-\varepsilon_{C\{i\}})^2} [C_D]^{\varepsilon_{C\{i\}}(1-\varepsilon_{C\{i\}})} \right. \\
& \left. + RT \ln \left([NH_3]^{\gamma_S(1-\varepsilon_{C\{i\}})^2} [N_D]^{\gamma_S\varepsilon_{C\{i\}}(1-\varepsilon_{C\{i\}})} \right) \right. \\
& \left. + RT \ln \left([H_3PO_4]^{\delta_S(1-\varepsilon_{C\{i\}})^2} [P_D]^{\delta_S\varepsilon_{C\{i\}}(1-\varepsilon_{C\{i\}})} \right) \right. \\
& \left. - RT \ln \left([S_{\chi\{j\}}] [C_{\chi\{j\}}]^{[C_{\chi\{j\}}]/[X\{j\}]} [O_2(aq)]^{a_{C\{i\}}^c(1-\varepsilon_{C\{i\}})} \right).
\end{aligned} \tag{S55}$$

210 The electrons transferred in catabolic sub-reaction of $R_{\chi\{j\},C\{i\}}$ is,

$$n_{C\{i\}}^e = 4. \tag{S56}$$

211 Consumer preference for prey $S_{\chi\{j\}}$, given by $\Omega_{\chi\{j\},C\{i\}}$, is weighted by all prey concentrations
212 that consumer $S_{C\{j\}}$ is allowed to eat is given by,

$$\Omega_{\chi\{j\},C\{i\}} = \frac{\Omega_{\chi\{j\},C\{i\}} [S_{\chi\{j\}}]}{\sum_j \Omega_{P\{j\},C\{i\}} [S_{P\{j\}}] + \sum_j \Omega_{B\{j\},C\{i\}} [S_{B\{j\}}] + \sum_j \Omega_{C\{j\},C\{i\}} [S_{C\{j\}}]}. \tag{S57}$$

213 The reaction rate, $r_{\chi\{j\},C\{i\}}$, of reaction $R_{\chi\{j\},C\{i\}}$ is,

$$\begin{aligned}
& r_{\chi\{j\},C\{i\}} \\
& = v^* \varepsilon_{C\{i\}}^2 \omega_{\chi\{j\},C\{i\}} [S_{C\{i\}}] \left(\frac{[S_{\chi\{j\}}]}{[S_{\chi\{j\}}] + \kappa^* \varepsilon_{C\{i\}}^4} \right) \left(\frac{[O_2(aq)]}{[O_2(aq)] + \kappa^* \varepsilon_{C\{i\}}^4} \right) F_T (\Delta_r G_{\chi\{j\},C\{i\}}, n_{C\{i\}}^e).
\end{aligned} \tag{S58}$$

214 Entropy production from reaction $R_{\chi\{j\},C\{i\}}$ and light absorption by $S_{C\{i\}}$ allocated to prey $\chi\{j\}$
215 is given by,

$$\dot{\sigma}_{\chi\{j\},C\{i\}}^R = -\frac{A\zeta_d}{T} r_{\chi\{j\},C\{i\}} \Delta_r G_{\chi\{j\},C\{i\}} \text{ and} \tag{S59}$$

$$\dot{\sigma}_{\chi\{j\},C\{i\}}^P = -\frac{A\zeta_d}{T} \langle I(t) \rangle_d \Delta_r G_\gamma k_p \Omega_{\chi\{j\},C\{i\}} [S_{C\{i\}}]. \tag{S60}$$

216 S2.3 Reaction Network, $\mathbf{S}(\mathbf{u})\mathbf{r}(t; \mathbf{u})$

217 The reaction network is defined by the stoichiometries of the reactions listed above. Instead of
 218 listing all the elements of the stoichiometric matrix, $\mathbf{S}(\mathbf{u})$, which is sparse, we list the n_S rows of the
 219 vector that results from the matrix vector product of $\mathbf{S}(\mathbf{u})\mathbf{r}(t; \mathbf{u})$, which is a mass balance around each
 220 state variable. For instance, $\mathbf{S}_{S_{P\{i\}}}^T \mathbf{r}$ is the net production rate of $S_{P\{j\}}$ resulting from the growth and
 221 predation. The rows of $\mathbf{S}(\mathbf{u})\mathbf{r}(t; \mathbf{u})$ are as follows:
 222

$$\begin{aligned} \mathbf{S}_{DIC}^T \mathbf{r} = & \sum_{i=1}^{n_P} \left(-\varepsilon_{P\{i\}} r_{1,P\{i\}} + \left(1 + \varepsilon_{P\{i\}} (n_{2,P\{i\}} - 1) \right) r_{2,P\{i\}} \right) \\ & + \sum_{i=1}^{n_B} \left(2 - \varepsilon_{B\{i\}} (a_{1,B\{i\}}^A + 1) \right) r_{1,B\{i\}} + \sum_{i=1}^{n_C} \sum_{j=1}^{n_P} \left((1 - \varepsilon_{C\{i\}})^2 + \frac{[C_{P\{j\}}]}{[S_{P\{j\}}]} \right) r_{P\{j\},C\{i\}} \\ & + \sum_{i=1}^{n_C} \sum_{j=1}^{n_B} (1 - \varepsilon_{C\{i\}})^2 r_{B\{j\},C\{i\}} + \sum_{i=1}^{n_C} \sum_{j=1}^{n_C} (1 - \varepsilon_{C\{i\}})^2 r_{C\{j\},C\{i\}}, \end{aligned} \quad (\text{S61})$$

$$\begin{aligned} \mathbf{S}_{O_2}^T \mathbf{r} = & \sum_{i=1}^{n_P} \left(\varepsilon_{P\{i\}} r_{1,P\{i\}} - \left(1 + \varepsilon_{P\{i\}} (a_{2,P\{i\}}^A + n_{2,P\{i\}} - 1) \right) r_{2,P\{i\}} \right) - \sum_{i=1}^{n_B} (1 - \varepsilon_{B\{i\}}) r_{1,B\{i\}} \\ & - \sum_{i=1}^{n_C} \sum_{j=1}^{n_P} \left(a_{C\{i\}}^C (1 - \varepsilon_{C\{i\}}) + \frac{[C_{P\{j\}}]}{[S_{P\{j\}}]} \right) r_{P\{j\},C\{i\}} - \sum_{i=1}^{n_C} \sum_{j=1}^{n_B} a_{C\{i\}}^C (1 - \varepsilon_{C\{i\}}) r_{B\{j\},C\{i\}} \\ & - \sum_{i=1}^{n_C} \sum_{j=1}^{n_C} a_{C\{i\}}^C (1 - \varepsilon_{C\{i\}}) r_{C\{j\},C\{i\}}, \end{aligned} \quad (\text{S62})$$

$$\mathbf{S}_{C_L}^T \mathbf{r} = \sum_{i=1}^{n_B} (-r_{1,B\{i\}} + r_{2,B\{i\}}), \quad (\text{S63})$$

$$\begin{aligned} \mathbf{S}_{C_D}^T \mathbf{r} = & - \sum_{i=1}^{n_B} r_{2,B\{i\}} + \sum_{i=1}^{n_C} \sum_{j=1}^{n_P} \varepsilon_{C\{i\}} (1 - \varepsilon_{C\{i\}}) r_{P\{j\},C\{i\}} + \sum_{i=1}^{n_C} \sum_{j=1}^{n_B} \varepsilon_{C\{i\}} (1 - \varepsilon_{C\{i\}}) r_{B\{j\},C\{i\}} \\ & + \sum_{i=1}^{n_C} \sum_{j=1}^{n_C} \varepsilon_{C\{i\}} (1 - \varepsilon_{C\{i\}}) r_{C\{j\},C\{i\}}, \end{aligned} \quad (\text{S64})$$

$$\begin{aligned} \mathbf{S}_{N_D}^T \mathbf{r} = & - \sum_{i=1}^{n_B} r_{3,B\{i\}} + \sum_{i=1}^{n_C} \sum_{j=1}^{n_P} \gamma_S \varepsilon_{C\{i\}} (1 - \varepsilon_{C\{i\}}) r_{P\{j\},C\{i\}} + \sum_{i=1}^{n_C} \sum_{j=1}^{n_B} \gamma_S \varepsilon_{C\{i\}} (1 - \varepsilon_{C\{i\}}) r_{B\{j\},C\{i\}} \\ & + \sum_{i=1}^{n_C} \sum_{j=1}^{n_C} \gamma_S \varepsilon_{C\{i\}} (1 - \varepsilon_{C\{i\}}) r_{C\{j\},C\{i\}}, \end{aligned} \quad (\text{S65})$$

$$\begin{aligned} \mathbf{S}_{NH_3}^T \mathbf{r} = & - \sum_{i=1}^{n_P} \varepsilon_{P\{i\}} \gamma_S r_{2,P\{i\}} + \sum_{i=1}^{n_B} (r_{3,B\{i\}} - \varepsilon_{B\{i\}} \gamma_S r_{1,B\{i\}}) + \sum_{i=1}^{n_C} \sum_{j=1}^{n_P} \gamma_S (1 - \varepsilon_{C\{i\}})^2 r_{P\{j\},C\{i\}} \\ & + \sum_{i=1}^{n_C} \sum_{j=1}^{n_B} \gamma_S (1 - \varepsilon_{C\{i\}})^2 r_{B\{j\},C\{i\}} + \sum_{i=1}^{n_C} \sum_{j=1}^{n_C} \gamma_S (1 - \varepsilon_{C\{i\}})^2 r_{C\{j\},C\{i\}}, \end{aligned} \quad (\text{S66})$$

$$\mathbf{S}_{S_{P\{i\}}}^T \mathbf{r} = \varepsilon_{P\{i\}} r_{2,P\{i\}} - \sum_{j=1}^{n_C} r_{P\{i\},C\{j\}}, \quad (\text{S67})$$

$$\mathbf{S}_{C_{P\{i\}}}^T \mathbf{r} = \varepsilon_{P\{i\}} r_{1,P\{i\}} - (1 + \varepsilon_{P\{i\}} n_{2,P\{i\}}) r_{2,P\{i\}} - \sum_{j=1}^{n_C} \frac{[C_{P\{i\}}]}{[S_{P\{i\}}]} r_{P\{i\},C\{j\}}, \quad (\text{S68})$$

$$\mathbf{S}_{S_{B\{i\}}}^T \mathbf{r} = \varepsilon_{B\{i\}} a_{1,B}^A r_{1,B\{i\}} - \sum_{j=1}^{n_C} r_{B\{i\},C\{j\}}, \quad (\text{S69})$$

$$\mathbf{S}_{S_{C\{i\}}}^T \mathbf{r} = \sum_{j=1}^{n_P} \varepsilon_{C\{i\}} r_{P\{j\},C\{i\}} + \sum_{j=1}^{n_B} \varepsilon_{C\{i\}} r_{B\{j\},C\{i\}} + \sum_{j=1}^{n_C} \varepsilon_{C\{i\}} r_{C\{j\},C\{i\}} - \sum_{j=1}^{n_C} r_{C\{i\},C\{j\}}. \quad (\text{S70})$$

223

224 S2.4 Integrated Entropy Production

225 Cumulative entropy production over the simulation (or optimization) interval is determined by
 226 summing then integrating the contributions of reactions, particle absorptions and water, as given by,
 227

$$\begin{aligned} \sigma^R = & \int_{t_0}^{t_f} \sum_{i=1}^{n_P} (\dot{\sigma}_{1,P\{i\}}^R(\tau) + \dot{\sigma}_{2,P\{i\}}^R(\tau)) d\tau + \int_{t_0}^{t_f} \sum_{i=1}^{n_B} (\dot{\sigma}_{1,B\{i\}}^R(\tau) + \dot{\sigma}_{2,B\{i\}}^R(\tau) + \dot{\sigma}_{3,B\{i\}}^R(\tau)) d\tau \\ & + \int_{t_0}^{t_f} \sum_{j=1}^{n_X} \sum_{i=1}^{n_C} \dot{\sigma}_{X\{j\},C\{i\}}^R(\tau) d\tau, \end{aligned} \quad (\text{S71})$$

228

$$\begin{aligned} \sigma^P = & \int_{t_0}^{t_f} \sum_{i=1}^{n_P} (\dot{\sigma}_{1,P\{i\}}^P(\tau) + \dot{\sigma}_{2,P\{i\}}^P(\tau)) d\tau + \int_{t_0}^{t_f} \sum_{i=1}^{n_B} (\dot{\sigma}_{1,B\{i\}}^P(\tau) + \dot{\sigma}_{2,B\{i\}}^P(\tau) + \dot{\sigma}_{3,B\{i\}}^P(\tau)) d\tau \\ & + \int_{t_0}^{t_f} \sum_{j=1}^{n_X} \sum_{i=1}^{n_C} \dot{\sigma}_{X\{j\},C\{i\}}^P(\tau) d\tau \text{ and} \end{aligned} \quad (\text{S72})$$

229

$$\sigma^W = \int_{t_0}^{t_f} \dot{\sigma}^W(\tau) d\tau. \quad (\text{S73})$$

230

231 The total entropy production used in the optimization described below is simply the sum,
 232

$$\sigma^T = \sigma^R + \sigma^W + \sigma^P. \quad (\text{S74})$$

233

234 S2.5 Initial Value Problem Integration

235 The numerical package BiM [8], which uses blended implicit methods to integrate stiff ordinary
 236 differential equations (ODEs), was used to solve the initial value problem (Eqn. S1) and to determine
 237 cumulative entropy production, Eqn. (S71-S74). All simulations were run for two years, 10^{-6} was used
 238 for both absolute and relative tolerances, a maximum step size (*hmax*) of 0.05 was implemented to
 239 insure diel light cycles were not stepped over, *maxstep* was increased to 10000000, and finite
 240 differences were used to calculate the Jacobian matrix. Default values were used for all other BiM
 241 options.

242 S3 Optimization of Trait-Based Model

243 Instead of employing optimal control to determine how $\varepsilon_{\mathcal{X}\{i\}}$ and $\Omega_{j,\mathcal{X}\{i\}}$ vary over time as has
 244 been previously used [2,9], in this manuscript we investigated a hybrid between MEP optimization
 245 and trait-based modeling. In typical trait-based models [1], a large number of each functional group
 246 are included in the model, and the traits, (i.e., $\varepsilon_{\mathcal{X}\{i\}}$ and $\Omega_{j,\mathcal{X}\{i\}}$) are randomly assigned values. When
 247 a simulation is run, organisms that grow fastest under the prevailing simulated environment
 248 dominate, while others are effectively culled from the population in a manner analogous to natural
 249 selection, but *in silico*. In order to explore the trait space, a large population of each functional group
 250 is needed; however, this presents a problem in our current model formulation. As the population size
 251 of \mathbb{S}_P and \mathbb{S}_B are increased, the column dimension of the predation matrix, $\Omega_{\mathcal{X}\{j\},C\{i\}}$, increases, so
 252 that the total number of traits in the model, given by $n_T = 2n_P + 3n_B + (1 + n_P + n_B + n_C)n_C$,
 253 increases rapidly with population size. For instance, a model with just 10 ecotypes in each functional
 254 group has 360 trait values in total, and one with 100 ecotypes each has 30,600 trait values in total; the
 255 size of the trait space scales with $O(n^2)$. One way to circumvent the scaling problem is to limit the
 256 number of prey each consumer can target, but this places more constraints on the structure of the
 257 food web than we desired. While we investigated the standard trait-based approach, we found the
 258 $O(n^2)$ scaling on trait space made the approach untenable for our objectives; consequently, we
 259 developed a new, hybrid approach.

260 Instead of randomly assigning trait values, the hybrid approach numerically searches for trait
 261 values that maximize the objective function, in this case total entropy production. This approach does
 262 not require a large number of ecotypes of each functional group, because the trait space is not being
 263 explored randomly, but systematically using optimization. Even simulations with just one instance
 264 of each functional group ($n_T = 9$) generated reasonable solutions. In fact, as discussed in the main
 265 text, adding food web complexity in the form of more ecotypes did significantly increase EP in many
 266 of our 0D simulations. The hybrid approach differs from the optimal control approach in that neither
 267 $\varepsilon_{\mathcal{X}\{i\}}$ nor $\Omega_{j,\mathcal{X}\{i\}}$ vary during a simulation. Consequently, the size/complexity of the food web likely
 268 needs to be larger for temporally and spatially varying environments in order to cover all niches, but
 269 time varying environments, other than light intensity, were not investigated in this study. Once optimal
 270 parameter values are determined for a given set of environmental conditions, the optimization
 271 component does not need to be rerun.

272 S3.1 hyperBOB

273 For the optimization, we used the derivative-free, box-constrained, local optimizer BOBYQA[10]
 274 to search the n_T dimensional trait space by maximizing σ^T defined by Eqns. (S71-S74). To search
 275 for a global optimum on a computer cluster with N_{CPU} CPUs, BOBYQA was started with N_{CPU}
 276 different initial conditions that were selected by sampling from a Latin unit hypercube [11], which
 277 we implemented in the routine hyperBOB (DOI: [10.5281/zenodo.3978689](https://doi.org/10.5281/zenodo.3978689)). Parameters used in
 278 BOBYQA/hyperBOB were: *rhobeg*, 0.49; *rhoend*, 0.0001; *maxfun*, 10,000. Except on rare occasions,
 279 solutions were found before the maximum number of function calls (*maxfun*) occurred. A time
 280 constraint was also placed on the solution, but it also seldom was invoked. All simulations were run
 281 on a 5-node computer cluster with a total of 90 CPU cores.

282 S3.2 Temporal Strategies for Phytoplankton

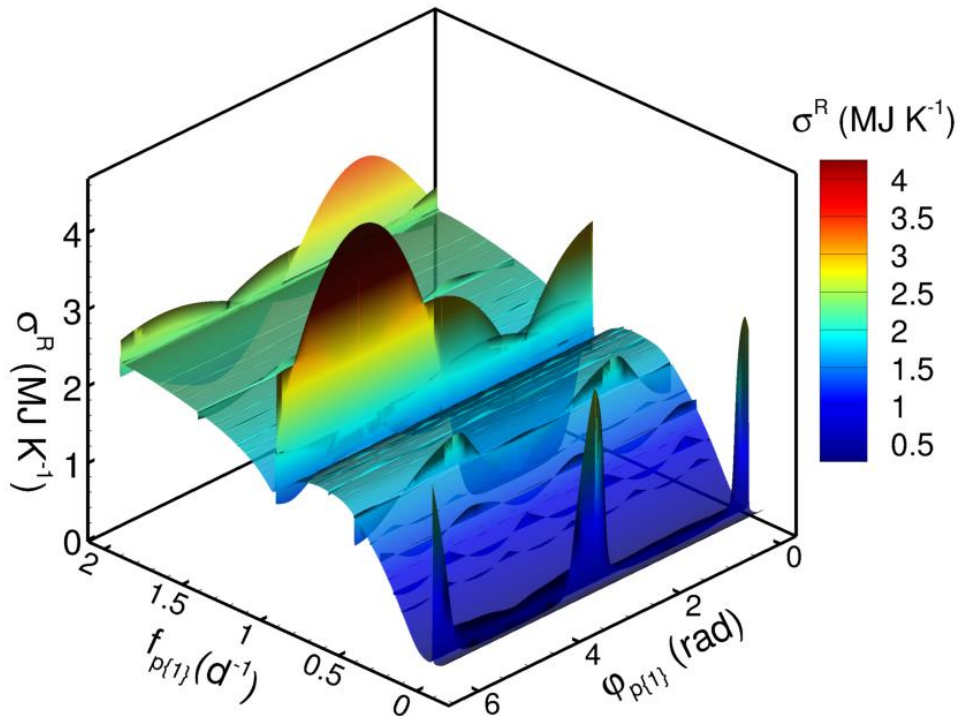
283 To investigate how temporal strategies, in particular circadian rhythms, increase entropy
 284 production, we used two different approaches. In the first approach that was later retired, the
 285 constant trait value assigned to $\Omega_{1,P\{i\}}$ was replaced by a time varying function that depends to two
 286 new trait variables, $f_{P\{i\}}$ and $\varphi_{P\{i\}}$, as given by,
 287

$$288 \Omega_{1,P\{i\}}(t) = \frac{1}{2} \left(\sin(2\pi f_{P\{i\}} t + \varphi_{P\{i\}}) + 1 \right), \quad (S75)$$

289 where $f_{P\{i\}}$ is the frequency $[[d^{-1}]]$ and $\varphi_{P\{i\}}$ the phase $[[rad]]$ of $\Omega_{1,P\{i\}}(t)$ that controls allocation
 290 of phytoplankton protein to CO₂ fixation given by reaction $R_{1,P\{i\}}$. When $f_{P\{i\}} = 0$, $\varphi_{P\{i\}}$ modifies the
 291 amplitude of $\Omega_{1,P\{i\}}$, but does not change over time. These two traits had the following bounds,
 292

$$0 \leq f_{P\{i\}} \leq 2 \text{ and } 0 \leq \varphi_{P\{i\}} \leq 2\pi. \tag{S76}$$

293
 294 Several simulation studies were conducted with the above temporal modification of $\Omega_{1,P\{i\}}(t)$;
 295 however, by allowing the frequency parameter to be a trait variable, we found that locating the global
 296 optimum proved challenging as evident in Figure S1, in which all traits were held constant for a
 297 1P1B1C simulation and σ^R was calculated for different values of $f_{P\{1\}}$ and $\varphi_{P\{1\}}$ at high resolution
 298 (1051 uniform samples in each dimension). Even though local optima occur for other frequencies, all
 299 simulations investigated showed the global optimum only occurred for $f_{P\{1\}} = 1 d^{-1}$; consequently,
 300 we used a different function for $\Omega_{1,P\{i\}}(t)$ in which frequency was fixed to the diel cycle of 1 per day
 301 to improve computational speed.



302
 303 Figure S1. Reaction entropy production, σ^R , for different values of $f_{P\{1\}}$ and $\varphi_{P\{1\}}$ for Eqn. (S75)
 304 while all other traits held constant for a 1P1B1C food web model. Note, the global optimum is
 305 located at a frequency of 1 d⁻¹; however, the peak is very narrow and was often missed by the
 306 hyperBOB search algorithm unless constraints on $f_{P\{1\}}$ were centered near 1.

307 For all simulations described in the main text, the following time varying square wave function
 308 for $\Omega_{1,P\{i\}}(t)$ was used instead of Eqn. (S75),
 309

$$\Omega_{1,P\{i\}}(t) = \Omega_{amp\{i\}} \max(\delta_S(\text{mod}(t, 1), t_{On\{i\}}, \lambda_s) + \delta_S(\text{mod}(t, 1), t_{Off\{i\}}, -\lambda_s) - 1, 0), \tag{S77}$$

310
 311 where $\delta_S(t, t_s, \lambda_s)$ is a smooth unit step function around t_s given by,
 312

$$\delta_S(t, t_s, \lambda_s) = \frac{1}{e^{-\lambda_s(t-t_s)} + 1}. \tag{S78}$$

313
 314 In Eqn. (S77), three parameters, all bounded between 0 and 1, govern the characteristics of the
 315 $\Omega_{1,P\{i\}}(t)$ square-wave step function that occurs each day: $t_{on\{i\}}$ specifies time of day when the step-
 316 up occurs; $t_{off\{i\}}$ specifies when the step-down occurs; $\Omega_{amp\{i\}}$ specifies the amplitude of the step.
 317 The parameter λ_s was not considered a trait, but rather is used to control numerical smoothness of
 318 the step and was set to a value of 200 d⁻¹ for all simulations. For either Eqn. (S75) or (S77), since
 319 biomass allocation must be conserved, $\Omega_{2,P\{i\}}(t)$ is obtained from the difference given by 1 –
 320 $\Omega_{1,P\{i\}}(t)$.

321 One of the three types of temporal strategies discussed in the main text examines the impact of
 322 strict balanced growth for phytoplankton, so that the C:N ratio of phytoplankton remains constant
 323 (technically, this is a no-temporal-strategy strategy). To achieve balanced growth, $r_{1,P\{i\}}$ must be
 324 coupled to $r_{2,P\{i\}}$ so that the ratio of $S_{P\{i\}}$ concentration to $C_{P\{i\}}$ concentration remains constant, or
 325 that,
 326

$$\frac{d[C_{P\{i\}}]/[S_{P\{i\}}]}{dt} = 0, \quad (S79)$$

327
 328 which occurs when,
 329

$$\frac{r_{1,P\{i\}}(t)}{r_{2,P\{i\}}(t)} = \beta_{P\{i\}} \stackrel{\text{def}}{=} \left(\frac{1}{\varepsilon_{P\{i\}}} - n_{2,P\{i\}} + k_{PP\{i\}} \right), \quad (S80)$$

330
 331 where $k_{PP\{i\}}$ is a specified constant that sets the ratio's $[C_{P\{i\}}]/[S_{P\{i\}}]$ value, which was set to 1 for
 332 all balance growth simulations. In simulations with balanced growth (i.e., no temporal strategy),
 333 $r_{1,P\{i\}}(t)$ and $r_{2,P\{i\}}(t)$ are calculated based on Eqns. (S12) and (S26), respectively, then adjusted as
 334 follows,
 335

$$r_{1,P\{i\}}(t) = \min\left(r_{1,P\{i\}}(t), \beta_{P\{i\}} r_{2,P\{i\}}(t)\right) \text{ and} \quad (S81)$$

336

$$r_{2,P\{i\}}(t) = \min\left(r_{2,P\{i\}}(t), \frac{1}{\beta_{P\{i\}}} r_{1,P\{i\}}(t)\right). \quad (S82)$$

337
 338 For example, at night, $r_{1,P\{i\}}(t)$ is zero and Eqn. (S82) forces $r_{2,P\{i\}}(t)$ to zero. Similarly, if no NH₃ is
 339 present, so that $r_{2,P\{i\}}(t)$ equals zero, then $r_{1,P\{i\}}(t)$ is set to zero based on Eqn. (S81) and
 340 phytoplankton dissipate solar radiation as particles, as described in Section S2.2.1 above.
 341

342 Simulations in the main text were conducted with version 4.7 of the model, which can be obtained
 343 from GitHub (DOI: [10.5281/zenodo.3979922](https://doi.org/10.5281/zenodo.3979922)).
 344

345 S4 Example parameter input file

346 Below is the parameter file used for the circadian clock strategy at a dilution rate of 0.2 d⁻¹ using
 347 the nominal input concentrations given in Table 2 of the main text.
 348

```
349 ! Run149_opt4.5_lplb1c
350 ! Using AutoHetDet_Opt_V4.5
351 ! 16-Jun-2020 on MEP
```

```

352 ! This is Run149, but using V4.5.
353 ! three parameters to specify a square wave function for omg_pp
354
355 &params
356 ! Input parameters
357 npp = 1 ! number of S1 primary producers
358 nbac = 1 ! number of bacteria
359 ncc = 1 ! number of S2 consumers
360
361 ! sumSigWeights determines which EP terms to use for optimization.
362 ! Weights on EP where vector is: [Rxns, H2O, particles]
363 ! Total EP production use 1., 1., 1., for just rxn, use 1., 0., 0., etc.
364 sumSigWeights = 1., 1., 1.
365
366 ! These parameters are used for EP surface generation only.
367 genSurf = .false. ! Should an EP surface be generated instead of optimization
368 readeps = .false. ! Read in the trait values from file.
369 whichPP = 1 ! which of the possible pp's to run f_pp and phi_pp over
370 nSurfPts = 1051 ! Number of points in the x and y dimension of the 2D surface to produce
371 reportTime = 10. ! How often to update screen during problem (min).
372
373 iseed = 10 ! changing this value to produce a different set of random values.
374 nuStar = 350. ! Used in adaptive Monod equation 1/d
375 nuDet = 175. ! For detritus decomp (1/d)
376 kappa = 5000. ! Adaptive Monod equation universal parameter (uM)
377 surA = 1.0 ! surface area of pond (m^2).
378 T_K = 293. ! get temperature (K)
379 pH = 8.1 ! pH
380 depth = 1.0 ! Pond depth (m)
381 is = 0.72 ! Ionic strength (M) = 0.72*sal/35.0 (sal is salinity (PSU))
382 dil_t0 = 0.2 ! dilution rate at t0 (1/d)
383 dil_tf = 0.2 ! dilution rate at tf (1/d)
384 dil_n = 0 ! number of steps in dilution rate between t0 and tf
385
386 ! Parameters associated with in-silico selection of traits
387 minCompFac = 500000.0 ! If process takes longer than (tf-t0)/minCompFac, then terminate
388 epp_min = 0.00001 ! min and max values for epp
389 epp_max = 1.0
390 ecc_min = 0.00001 ! min and max values for ecc
391 ecc_max = 1.0
392 ebac_min = 0.0001 ! min and max values for ebac
393 ebac_max = 1.0
394
395 ! limits and parameters
396 ! The square wave is limited to occur every day, so frequency is fixed in V4.0 and later
397 ! tOn_pp is when the step up occurs, and tOff_pp when steps down occurs. These are in days.
398 ! Note, the overhangs (< 0 on tOn and >1 on tOff) insures omg_pp can be fully on all day
399 ! because of the nature of the exp step function and value of sigOmg_pp.
400 ! These are used for circadian strategy
401 sigOmg_pp = 200. ! this is used in the exp setup function to make a "smooth" square wave
402 tOn_pp_min = -0.05 ! lower limit on on time (d)
403 tOn_pp_max = 1.0 ! upper limit when step up can occur (d)
404 tOff_pp_min = 0.0 ! lower limit when a step down can occur (d)
405 tOff_pp_max = 1.05 ! upper limit when step down occurs (d)

```

```

406 ! Use these for no circadian rhythm (i.e., passive storage).
407 ! tOn_pp_min = -0.05 ! lower limit on on time (d)
408 ! tOn_pp_max = -0.049 ! upper limit when step up can occur (d)
409 ! tOff_pp_min = 1.04 ! lower limit when a step down can occur (d)
410 ! tOff_pp_max = 1.05 ! upper limit when step down occurs (d)
411
412 ! V4.7 Add binaryOMG to set omg_cc to binary matrix (only 0's or 1's)
413 binaryOMG = .false. ! default is .false.
414
415 ! Coupling between r_1,p and r_2,p. If k_pp below is set to zero (default) then
416 ! reactions are not coupled, but if k_pp > 0, then it sets the ratio of
417 ! C_p to p (i.e., C_p/p = k_pp). Note, there is also the variable k_p for light
418 ! attenuation that is different. When k_pp /= 0, tOn_pp and tOff_pp should be set to
419 ! the passive storage scenario.
420 k_pp = 0.0
421
422 ! Initial and feed concentrations in input feed. All concentrations in uM
423 dicI = 2000. ! (uM)
424 o2I = 225. ! (uM)
425 nh3I_t0 = 5. ! nh3I at t0 (uM)
426 nh3I_tf = 5. ! nh3I at tf (uM)
427 nh3I_n = 0 ! Number of steps in nh3I between t0 and tf
428 c_LI = 10. ! labile carbon (uM)
429 c_dI = 100.0 ! detrital carbon (uM)
430 n_dI = 7. ! detrital nitrogen (uM)
431 ppI = 0.1 ! initialize all phytoplankton to this value (uM)
432 c_ppI = 0.1 ! all phytoplankton carbon stores (uM)
433 ccI = 0.1 ! initialize all consumers to this value (uM)
434 bacI = 0.1 ! all bacteria (uM)
435
436 ! Phosphate concentrations. Held fixed, but used for thermodynamic calculations
437 h3po4 = 1. ! uM
438 P_d = 5. ! detrital P (uM)
439
440 ! Biomass elemental composition. From Battley1998 for yeast. Unit carbon
441 alf = 1.613 ! H
442 bet = 0.557 ! O
443 gam = 0.158 ! N
444 del = 0.012 ! P
445 cell_F = 1000.0 ! concentration factor for C_P. Intracellular versus extracellular volume.
446 delPsi = 0.1 ! LaRowe's thermo driver. Cell membrane potential (V)
447
448 ! Gas Exchange, temp and pH
449 pV_o2 = 3.0 ! piston velocity for O2 (m/d)
450 pV_co2 = 2.6 ! piston velocity for CO2 (m/d)
451 pO2 = 0.21 ! partial pressure of O2 in atmosphere (atm)
452 pCO2 = 400.d-6 ! partial pressures CO2 in the atmosphere (atm)
453
454 ! Solar parameters
455 I0max = 406000. ! Solar constant in PAR (mmol photons /m^2 /d)
456 dLat = 42.0 ! Latitude for calculating solar radiation
457 dGr_Ggamma = -253. ! Gibbs free energy of photons (J/mmol photon of blue light, 440 nm)
458 k_w = 0.011 ! water attenuation coef (1/m) (see Table 2.11 of Wozniak2007 for 430 nm light)
459 k_p = 0.000625 ! attenuation coef by non-algal parties (m^2/mmol-S)

```

```

460 k_chla = 0.0025 ! attenuation coef by algal pigments. (Wozniak2007, adjusted to (m^2/mmol-S))
461
462 ! BiM ODE solution parameters
463 ompThreads = 1 ! Specify how many threads to use (no currently used, set to 1)
464 t0 = 0. ! Start time for ODE integration (d)
465 tDays = 730. ! number of days to run simulation (d)
466 t0_ep = 0. ! For optimization, interval over which EP production is maximized.
467 tf_ep = 730. ! end of EP interval.
468 maxstep_BiM = 1000000 ! maximum number of BiM iterations (set to 0 to use default of 100000)
469 useOmpJac = 0 ! set to 0 to have BiM calculate numerical gradient
470 maxattempts = 1 ! number of attempts to solve ODEs before declaring failure
471 absZero = 1.e-8 ! Numbers less than this are set to this value smoothly. (div by 0 prevention)
472 atol1 = 1.0e-6 ! absolute tolerance for BiM
473 rtol1 = 1.0e-6 ! relative tolerance for BiM
474 hmax_BiM = 0.05 ! largest step size (d). default = (TEND-T0)/8
475
476 ! parameters used by hyperBOB
477 rhobeg = 0.49 ! initial and final values of a trust region radius
478 rhoend = 0.0001 ! When trust region is less than rhoend, stop.
479 iprint = 0 ! controls amount of printing (0, 1, 2 or 3)
480 maxfun = 10000 ! maximum number of calls to CALFUN
481 optimize = .true. ! If true, MEP optimization occurs, otherwise just solve ODEs
482 fcnUpdate = 100 ! output current status after every fcnUpdate ODE integrations
483 /
484

```

485 S5 References

- 486 1. Follows, M.J.; Dutkiewicz, S.; Grant, S.; Chisholm, S.W. Emergent Biogeography of Microbial
487 Communities in a Model Ocean. *Science* **2007**, *315*, 1843-1846, doi:10.1126/science.1138544.
- 488 2. Vallino, J.J.; Huber, J.A. Using Maximum Entropy Production to Describe Microbial Biogeochemistry
489 Over Time and Space in a Meromictic Pond. *Frontiers in Environmental Science* **2018**, *6*, 1-22,
490 doi:10.3389/fenvs.2018.00100.
- 491 3. Brock, T.D. Calculating solar radiation for ecological studies. *Ecol.Model.* **1981**, *14*, 1-19.
- 492 4. Alberty, R.A. *Thermodynamics of biochemical reactions*; Wiley & Sons: Hoboken, NJ, 2003.
- 493 5. LaRowe, D.E.; Dale, A.W.; Amend, J.P.; Van Cappellen, P. Thermodynamic limitations on microbially
494 catalyzed reaction rates. *Geochimica et Cosmochimica Acta* **2012**, *90*, 96-109, doi:10.1016/j.gca.2012.05.011.
- 495 6. Wozniak, B.; Dera, J. *Light absorption in sea water*; Springer: 2007; Vol. 33, pp. 463.
- 496 7. Candau, Y. On the exergy of radiation. *Solar Energy* **2003**, *75*, 241-247, doi:10.1016/j.solener.2003.07.012.
- 497 8. Brugnano, L.; Magherini, C. The BiM code for the numerical solution of ODEs. *Journal of Computational*
498 *and Applied Mathematics* **2004**, *164-165*, 145-158, doi:10.1016/j.cam.2003.09.004.
- 499 9. Vallino, J.J.; Algar, C.K.; González, N.F.; Huber, J.A. Use of Receding Horizon Optimal Control to Solve
500 MaxEP-Based Biogeochemistry Problems. In *Beyond the Second Law - Entropy production and non-*
501 *equilibrium systems*, Dewar, R.C., Lineweaver, C.H., Niven, R.K., Regenauer-Lieb, K., Eds. Springer
502 Berlin Heidelberg: 2014; 10.1007/978-3-642-40154-1_18pp. 337-359.
- 503 10. Powell, M.J. *The BOBYQA algorithm for bound constrained optimization without derivatives*; Cambridge NA
504 Report NA2009/06; University of Cambridge: Cambridge, 2009; pp 26-46.

- 505 11. McKay, M.D.; Beckman, R.J.; Conover, W.J. A Comparison of Three Methods for Selecting Values of
506 Input Variables in the Analysis of Output from a Computer Code. *Technometrics* **1979**, *21*, 239-245,
507 doi:10.2307/1268522.

508

509



© 2020 by the authors. Submitted for possible open access publication under the terms and conditions of the Creative Commons Attribution (CC BY) license (<http://creativecommons.org/licenses/by/4.0/>).

510